www.sciencemag.org/content/348/6238/1007/suppl/DC1

Supplementary Material for

Engram cells retain memory under retrograde amnesia

Tomás J. Ryan, Dheeraj S. Roy, Michele Pignatelli, Autumn Arons, Susumu Tonegawa*

*Corresponding author. E-mail: tonegawa@mit.edu

Published 29 May 2015, *Science* **348**, 1007 (2015)
DOI: 10.1126/science.aaa5542

This PDF file includes:

Materials and Methods

Subjects

All experiments were conducted in accordance with U.S. National Institutes of Health guidelines and the Massachusetts Institute of Technology Department of Comparative Medicine and Committee of Animal Care. c-fos-tTA transgenic mice were generated as described in (16), by breeding TetTag mice (22) with C57BL/6J mice and selecting offspring carrying only the c-fos-tTA transgene. Mice had access to food and water *ad libitum* and were socially housed in numbers of two to five littermates until surgery. Following surgery, mice were singly housed. For behavioral experiments, all mice used for the experiments were male and 7–9 weeks old at the time of surgery and had been raised on food containing 40 mg kg^{-1} doxycycline (DOX) for at least one week before surgery, and remained on DOX food for the remainder of the experiments except for the target engram labeling days. For *ex vivo* electrophysiology experiments, mice were 24-28 days old at the time of surgery.

Engram labeling strategy

In order to label memory engram cells, we employed adeno-associated viruses that express either mCherry alone or ChR2 fused to an EYFP/mCherry fluorophore under the control of a tetracycline-responsive element (TRE)-containing promoter (AAV_9-TRE-mCherry, AAV_9-TRE-ChR2-EYFP, or AAV_9-TRE-ChR2-mCherry), which are active in cells that contain the tetracycline transactivator (tTA) (16). For each engram experiment, we injected one of these viruses into the target brain region of c-fos-tTA transgenic mice, which express tTA under the control of a *c-fos* promoter (fig. S1A) (22). Because *c-fos* is an activity-dependent gene, the c-fos-tTA transgene selectively expresses tTA in active cells (fig. S1B). Thus, active cells can express tTA that will then induce the virus to express mCherry or ChR2 in those cells. In order to restrict activity-dependent labeling to targeted training episodes the mice were fed DOX food, which sequesters tTA function and prevents virus expression. Subjects were then taken Off DOX one day prior to training in order to permit the labeling of memory engram cells (fig. S1C, D, E). Shining 473 nm blue light on a ChR2 positive neuron causes the opening of ChR2 channels, and the rapid influx of cations results in the depolarization of the neuron (41). Therefore, by shining blue light onto ChR2-labeled engram cells, memory recall can be directly evoked (16). Patch-clamp recordings *in vitro* confirmed that light successfully activated ChR2-labeled DG cells following contextual fear conditioning (CFC) (fig. S1F, G).

Virus-mediated gene expression

The recombinant AAV vectors used for viral production were pAAV-TRE-ChR2-EYFP described in (16), pAAV-TRE-ChR2-mCherry and pAAV-TRE-mCherry described in (17). The pAAV-hSyn1-HA-hM4Di-IRES-mCitrine plasmid was acquired from Bryan Roth at the University of North Carolina. The pAAV-CaMKIIα-ChR2-EYFP plasmid was acquired from Addgene. Plasmids were serotyped with AAV_8 or AAV_9 coat proteins and packaged at the University of Massachusetts Medical School Gene Therapy Center and Vector Core.
The recombinant AAV vectors were injected with viral titers of 1 X 10^{13} genome copy (GC) ml^{-1} for AAV_9-TRE-ChR2-EYFP, 8.0 × 10^{12} GC ml^{-1} for AAV_9-TRE-ChR2-mCherry, 1.4 X 10^{13} GC ml^{-1} for AAV_9-TRE- mCherry, 3.3 X 10^{12} GC ml^{-1} for AAV_9-hSyn1-HA-hM4Di-IRES-mCitrine, and 8.0 X 10^{12} GC ml^{-1} for AAV_8-CaMKIIα-ChR2-EYFP.

Stereotactic surgery procedure

Mice were anesthetized using 500 mg kg^{-1} avertin, or isoflurane. Bilateral craniotomies were performed using a 0.5 mm diameter drill and the viruses were injected using a glass micropipette attached to a 10 ml Hamilton microsyringe (701LT; Hamilton) through a microelectrode holder (MPH6S; WPI) filled with mineral oil. A microsyringe pump (UMP3; WPI) and its controller (Micro4; WPI) were used to maintain the speed of the injection at 60 nl min^{-1}. The needle was slowly lowered to the target site and remained for 5 min before beginning the injection. After the injection, the needle stayed for 10 minutes before it was slowly withdrawn. After withdrawing of

the needle, a custom implant containing two optic fibers (200 mm core diameter; Doric Lenses) was lowered above the injection site. Two jewelry screws were screwed into the skull on either side of bregma. A layer of adhesive cement (C&B Metabond) was applied followed with dental cement (Teets cold cure; A-M Systems) to secure the optic implant. A cap derived from the top part of an Eppendorf tube was inserted to protect the implant. Mice were given 1.5 mg kg^{-1} metacam as analgesic and remained on a heating pad until fully recovered from anesthesia. Mice were allowed to recover for at least 2 weeks before all subsequent behavioral experiments.

Ex vivo patch clamp recording

Stereotactic surgery

For AMPA/NMDA ratio experiments (Fig. 1A-E), entorhinal cortex (EC) injections of AAV_8-CaMKIIα-ChR2-EYFP (500 nl) were targeted unilaterally to (-4.7 mm anteroposterior (AP), +3.35 mm mediolateral (ML), - 3.3 mm dorsoventral (DV)), and dentate gyrus (DG) injections of AAV_9-TRE-mCherry (300 nl) were targeted unilaterally to (-2.0 mm AP, +1.3 mm ML, –1.9 mm DV).
For experiments involving spine counting (Fig. 1F, fig. S6, and fig. S7) and intrinsic physiological properties (fig. S4, fig. S6, and fig. S7), injections of AAV_9-TRE-ChR2-EYFP (300 nl) were targeted unilaterally to (-2.0 mm AP, +1.3 mm ML, –1.9 mm DV).
For fig. S4, DG injections of AAV_8-CaMKIIα-ChR2-EYFP (300 nl) were targeted unilaterally to (-2.0 mm AP, +1.3 mm ML, –1.9 mm DV).
For DG-CA3 connectivity experiments (Fig. 1G), DG injections of AAV_9-TRE-ChR2-EYFP (100 nl) were targeted unilaterally to (-2.0 mm AP, +1.3 mm ML, –1.9) mm DV, and CA3 injections of AAV_9-TRE-mCherry (150 nl) were targeted unilaterally to (-2.0 mm AP, +2.3 mm ML, –2.2 mm DV).

Animals and slice preparation

All *ex vivo* experiments were conducted blind to experimental group. Researcher 1 trained the animals and administered drug, while Researcher 2 dispatched the animals and conducted physiological experiments. Mice (P30-P40) were anesthetized with isoflurane, decapitated and brains were quickly removed. Sagittal slices (300 μm thick) were prepared in an oxygenated cutting solution at ~4°C by using a vibratome (VT1000S, Leica). Slices were then incubated at room temperature (~23°C) in oxygenated ACSF until the recordings. The cutting solution contained (in mM): 3 KCl, 0.5 $CaCl_2$, 10 $MgCl_2$, 25 $NaHCO_3$, 1.2 NaH_2PO_4, 10 D-glucose, 230 sucrose, saturated with 95%O_2 - 5%CO_2 (pH 7.3, osmolarity 340 mOsm). The ACSF contained (in mM): 124 NaCl, 3 KCl, 2 $CaCl_2$, 1.3 $MgSO_4$, 25 $NaHCO_3$, 1.2 NaH_2PO_4, 10 D-glucose, saturated with 95%O_2 - 5% CO_2 (pH 7.3, osmolarity 300 mOsm). Individual slices were transferred into a submerged experimental chamber and perfused with oxygenated ACSF warmed at 35°C (±0.5°C) at a rate of 3 ml/min during recordings.

Electrophysiology

Whole cell recordings in current clamp or voltage clamp mode were performed by using an IR-DIC microscope (BX51, Olympus) with a water immersion 40X objective (N.A. 0.8), equipped with four automatic manipulators (Luigs & Neumann) and a CCD camera (Orca R2, Hamamatsu Co). For all the recordings, borosilicate glass pipettes were fabricated (P97, Sutter Instrument) with resistances of 8 to 10 MΩ. For current clamp recordings, pipettes were filled with the following intracellular solution (in mM): 110 K-gluconate, 10 KCl, 10 HEPES, 4 ATP, 0.3 GTP, 10 phosphocreatine and 0.5% biocytin. The osmolarity of this intracellular solution was 290 mOsm and the pH was 7.25. The AMPA/NMDA ratio measurements were performed by adding 10 μM gabazine (Tocris) in the extracellular solution, and recordings in voltage clamp were performed by using the following intracellular solution (in mM): 117 cesium methansulfonate, 20 HEPES, 0.4 EGTA, 2.8 NaCl, 5 TEA-Cl, 4 Mg-ATP, 0.3 Na-GTP, 10 QX314, 0.1 spermine and 0.5% biocytin. The osmolarity of this intracellular solution was 290 mOsm and the pH was 7.3. Recordings were amplified using up to two dual channel amplifiers (Multiclamp 700B, Molecular Devices), filtered at 2 kHz, digitized (20 kHz), and acquired through an ADC/DAC data acquisition unit (ITC1600, Instrutech) by using custom made software running on Igor Pro (Wavemetrics). Access resistance (RA) was monitored throughout the duration of the experiment and data acquisition was suspended whenever the resting membrane

potential was depolarized above -50 mV or the RA was beyond 20 MΩ. All drugs used (Gabazine, NBQX, AP5, ANI) were provided by Tocris.

Optogenetics

Optogenetic stimulation was achieved through a 460 nm LED light source (XLED1, Lumen Dynamics) driven by TTL input with a delay onset of 25 µs (subtracted off-line for the estimation of latencies). Light power on the sample was 33 mW/mm^2. To test ChR2 expression, slices were stimulated with a single light pulse of 1 s, repeated 10 times every 5 s. To test synaptic connections, slices were stimulated with single light pulses of 2 ms, repeated 20 times every 5 s. In voltage clamp mode, cells were held at -70 mV, while in current clamp mode, response to optogenetic stimulation was measured at resting potential. DG-CA3 connectivity (Fig. 1G) was tested in current clamp mode, holding the cell at -70 mV. A train of 15 pulses at 20 Hz was delivered 20 times every 5 s and the average response was computed. The glutamatergic nature of the connection was confirmed by bath application of 10 µM NBQX (N = 4). The effect of ANI treatment on CA3 engram cells was evident from the measurement of the membrane capacitance (SAL: $mCherry^-$ 89.5 ± 7 pF, $mCherry^+$ 115 ± 9 pF, unpaired t test $P < 0.05$; ANI: $mCherry^-$ 103 ± 14 pF, $mCherry^+$ 95 ± 15 pF, unpaired t test $P = 0.7$).

Analysis

Synaptic connections, in voltage or current clamp mode, were determined by averaging 20 trials. EPSC amplitude was measured from the average maximum peak response by subtracting a baseline obtained 5 ms before light pulse starts (Fig. 1A-E). AMPA/NMDA ratios were measured in voltage clamp mode holding the voltage at -70 mV for AMPA current amplitude and holding the voltage at +40 mV for NMDA current amplitude measurement. The amplitude of the NMDA current was measured 100 ms after the onset of the light to avoid AMPA current overlap. The probability of DG-CA3 connectivity (Fig. 1G) was computed as, P = (successful tests/total test number). Error bars are approximated by binomial distribution. Spontaneous EPSCs (EPSCs) (fig. S2) were recorded at a holding potential of -70 mV in presence of Gabazine (10 µM). EPSCs were detected using an Igor Pro routine and were defined as inward currents with amplitudes exceeding two times the standard deviation of the baseline noise.
Granule cells expressing ChR2-EYFP, which in current clamp mode (at resting potential) responded to optogenetic stimulation with at least one action potential were considered engram cells and were selected for the analysis. The intrinsic electrophysiological properties (fig. S4) were measured in current clamp mode, holding the cell at –70 mV. Resting membrane potential was measured in current clamp mode without current injection. Action potential threshold was tested with a current ramp injection. Input resistance was measured by injecting a negative -120 pA current lasting 1 s. Membrane time constant was estimated through single exponential fit of the recovery-time from a –10 mV voltage deflection of 1 s duration. Excitability was estimated by linear fit of current (I) vs. firing rate (F) relationship.

Statistics

Statistical analysis was performed using Igor (Wavemetrics), MATLAB (Math works) or Excel (Microsoft). The distribution of the data was tested with the Kolmogorov-Smirnov test. A two sample Kolmogorov-Smirnov test, a Wilcoxon signed-rank test, a two-tailed paired or unpaired *t* test was employed for comparisons according to the application. Data are presented as mean ± SEM. To test significance of the connection probability, a Fisher's exact test was employed.

Post hoc immunocytochemistry

Recorded cells were filled with biocytin and subsequently recovered for morphological identification. Slices were first incubated with 4% PFA for 16 hr at 4°C. After washing with 0.5% Triton-X, slices were incubated in 5% normal goat serum (NGS) for 2 hr. Following NGS, slices were incubated in primary antibody (rabbit anti-RFP, 1:1000) overnight at 4°C. After washing with 0.5% Triton-X, slices were visualized by streptavidin CF633 (1:200, Biotium) and anti-rabbit Alexa-555. Before mounting, slices were incubated with DAPI (1:3000) for 30 min.

Spine density analysis

Experiments were conducted blind to experimental group. Researcher 1 imaged dendritic fragments, while Researcher 2 randomized images in advance of manual spine counting. Dentate granule cells were labeled with biocytin during patch clamp recordings. Fluorescence Z-stacks were taken by confocal microscopy (Zeiss LSM700), using 40 X objectives. Z-projected confocal images were generated by Zenblack (Zeiss). A total number of 16 granule cells were analyzed for spine examination (n = 4 cells per group x n = 4 groups). We analyzed 10 dendritic fragments of 10 µm length for each cell. To compute the spine density, the number of spines counted on each fragment was normalized by the cylindrical approximation of the surface of the specific fragment (Fig. 1F). The same applies for fig. S6, and fig. S7.

In vivo multi-unit electrophysiological recording

Using an anesthetized setup, multi-unit responses to optogenetic (ChR2) stimulation were recorded from c-fos-tTA mice injected with AAV_9-TRE-ChR2-EYFP virus in the DG. Mice were anesthetized by injection (10 ml kg^{-1}) of a mixture of ketamine (100 mg ml^{-1})/xylazine (20 mg ml^{-1}) and placed in the stereotactic system. Anesthesia was maintained by a series of booster doses of ketamine (100 mg kg^{-1}). An optrode consisting of a tungsten electrode (0.5 MΩ) attached to an optic fiber (200 µm core diameter), with the tip of the electrode extending beyond the tip of the fiber by 300 µm, was used for simultaneous optical stimulation and extracellular recording. The power intensity of light emitted from the optrode was calibrated to about 10 mW, which was consistent with the power intensity used in behavioral assays. To identify ChR2-positive cells, 15 ms light pulses at 0.2 Hz were delivered to the recording site every 50-70 µm. After light-responsive cells were detected, multi-unit activity in response to trains of 10 light pulses (15 ms) at 20 Hz was recorded. Activity was acquired using an Axon CNS Digidata 1440A system and analyzed using MATLAB, described in (17).

Behavior

Stereotactic injection and optic fiber implant

DG injections were targeted bilaterally to (-2.0 mm AP, +/- 1.3 mm ML, –1.9 mm DV). DG implants were placed at (-2.0 mm AP, +/- 1.3 mm ML, –1.9 mm DV). CA1 injections were targeted bilaterally to (-2.0 mm AP, +/- 1.5 mm ML, –1.5 mm DV). CA1 implants were placed at (-2.0 mm AP, +/- 1.5 mm ML, –1.4 mm DV). LA injections were targeted bilaterally to (-1.7 mm AP, +/- 3.45 mm ML, –4.2 mm DV). LA implants were placed at (-1.7 mm AP, +/- 3.45 mm ML, –4.0 mm DV). AAV_9-TRE-ChR2-EYFP volumes were 300 nl for DG and 500 nl for CA1. AAV_9-TRE-ChR2-mCherry volumes were 300 nl for DG and 200 nl for LA. AAV_9-hSyn1-HA-hM4Di-IRES-mCitrine volume was 500 nl for CA1. All injection sites were verified histologically. As criteria we only included mice with ChR2-EYFP or ChR2-mCherry expression limited to the targeted regions.

Optogenetics

For all DG and LA behavioral experiments, ChR2 was stimulated using a 473 nm laser delivering blue light at 20 Hz with a 15 ms pulse width, for the designated time period (16). For the CA1 experiment, 20 Hz proved ineffective (17), so here our stimulation protocol was adjusted to 4 Hz with a 15 ms pulse width.

Drug delivery

For consolidation experiments, 150 mg kg^{-1} anisomycin (ANI), or equivalent volume of saline (SAL), was delivered intra-peritoneally immediately after fear conditioning in the anteroom of the training context. For the ANI reconsolidation experiment, a second 150 mg kg^{-1} ANI dose was delivered 2 hours post-reactivation. For the cycloheximide (CHM) consolidation experiment 3 mg kg^{-1} CHM, or equivalent SAL, was delivered subcutaneously immediately after fear conditioning in the anteroom of the training context. For encoding experiments, 5 mg kg^{-1} clozapine-*N*-oxide (CNO) or SAL was delivered intra-peritoneally one hour before training, in the holding room.

Handling

All the behavioral experiments were conducted using mice that were 10 to 18 weeks of age, during the facility light cycle of the day (6.30 am to 6.30 pm). All behavioral subjects were individually habituated to handling by the investigator by handling for one minute on each of three separate days. Handling took place in the holding room where the mice were housed. Immediately prior to each handling session mice were transported by wheeled cart to and from the vicinity of the experimental context rooms, to habituate them to the journey.

Contextual Fear Conditioning – Consolidation (Figures 2A, 3B, 5A, S9, and S13)

Apparatus

For CFC experiments, two distinct contexts were employed, and used in different rooms. Context A chambers were 30 X 25 X 33 cm chambers with perspex floors, transparent square ceilings, red lighting, and scented with 0.25 % benzaldehyde. The ceilings of the Context A chambers were customized to hold a rotary joint (Doric Lenses) the exterior side of which was connected to a patch cord to a 473 nm laser that was controlled by a pulse generator. The interior side of the rotary joint was connected to two 0.32 M patch cords. All mice had patch cords fitted to the fiber implant prior to being placed in Context A. Two mice were run simultaneously in two identical Context A chambers. Context B chambers were 29 X 25 X 22 cm chambers with grid floors, opaque triangular ceilings, bright white lighting, and scented with 1 % acetic acid. Four mice were run simultaneously in four identical Context B chambers. All experimental groups were counter-balanced for chamber within contexts. All mice were conditioned in Context B, and tested in Contexts A and B. Experiments showed no generalization of conditioned response between contexts.

Floors of chambers were cleaned with Quatricide before and between runs. Mice were transported to and from the experimental room in their home cages using a wheeled cart. The cart and cages remained in an anteroom to the experimental rooms during all behavioral experiments.

Habituation

Four days prior to conditioning, all mice were habituated to Context A. Habituation sessions were 12 min in duration, consisting of four 3 min epochs, with the first and third epochs as the Light-Off epochs, and the second and fourth epochs as the Light-On epochs. During the Light-On epochs, the mouse received light stimulation (20 mW, 20 Hz, 15 ms) for the entire 3 min duration. At the end of 12 min, the mouse was immediately detached from the patch cords, returned to its home cage, and carted back to the holding room.

Training

Mice were trained in Context B using a CFC paradigm. Training sessions were 330 s in duration, and three 0.75 mA shocks of 2 s duration were delivered at 150 s, 210 s, and 270 s. SAL or ANI was delivered immediately after training. After fear conditioning, mice were placed in their home cages, and carted back to the holding room. Mice were kept on regular food without DOX for 24-30 hours prior to training. When training was complete, mice were switched back to food containing 40 mg kg^{-1} DOX.

Testing

All testing sessions in Context B were 180 s in duration. Testing conditions were identical to training conditioning, except that no shocks were presented. At the end of each session mice were placed in their home cages and carted back to the holding room.

All testing sessions in Context A were 12 min in duration, and were identical to the habituation sessions, consisting of four 3 min epochs, with the first and third epochs as the Light-Off epochs, and the second and fourth epochs as the Light-On epochs. During the Light-On epochs, the mouse received light stimulation (20 Hz for DG and LA, or 4 Hz for CA1) for the entire 3 min duration. At the end of 12 min, the mouse was immediately detached from the patch cords, returned to its home cage and carted back to the holding room.

Optogenetic Place Avoidance (OptoPA) - (Figure 3A)

Apparatus

Each OptoPA apparatus consisted of two distinct 15 × 15 × 20 cm zones (X and Y) connected to a triangular neutral zone as described in (17). . Zone X consisted of black and white striped walls and contained a transparent floor with small irregular indentations. Zone Y consisted of black and white alternating dotted walls and contained a smooth plastic floor. The wall of the neutral zone was customized to hold a rotary joint (Doric Lenses) the exterior side of which was connected to a patch cord to a 473 nm laser that was controlled by a pulse generator. The interior side of the rotary joint was connected to two 0.5 M patch cords. All mice had patch cords fitted to the fiber implant prior to being placed in the apparatus. Two mice were run simultaneously in two identical OptoPA apparatuses.

Training contexts were 29 X 25 X 22 cm chambers with grid floors, opaque triangular ceilings, red lighting, and scented with 1 % acetic acid. Four mice were run simultaneously in four identical chambers. All experimental groups were counter-balanced for chamber within contexts.

Habituation

All mice were habituated to the OptoPA apparatus and laser stimulation procedure 4 days prior to training (taken from (18)). Mice were allowed to freely explore both zones X and Y during the 0–3 min baseline epoch, and the naturally preferred zone was determined as the target zone. During the 3–6 min and 9–12 min epochs (Light-On phases), light was administered only when a mouse was within the target zone. At the end of the 12 min, the mouse was immediately detached from the patch cords, returned to its home cage and carted back to the holding room.

Training

Mice were trained using a contextual fear-conditioning paradigm. Training sessions were 500 s in duration, and four 0.75 mA shocks of 2 s duration were delivered at 198 s, 278 s, 358 s and 438 s. SAL or ANI was delivered immediately after training. After fear conditioning, mice were placed in their home cages, and carted back to the holding room. To enable engram labeling, mice were kept on regular food without DOX for 24-30 hours prior to training. When training was complete, mice were switched back to food containing 40 mg kg^{-1} DOX.

Testing

All mice were subjected to 180 s test sessions in the training context, 1 day post training. At the end of each session mice were placed in their home cages and carted back to the holding room.

OptoPA tests were conducted 2 days post training. Mice were allowed to freely explore both zones X and Y during the 0–3 min baseline epoch, and the naturally preferred zone was determined as the target zone. During the 3–6 min and 9–12 min epochs (Light-On phases), light was administered only when a mouse was within the target zone. At the end of the 12 min, the mouse was immediately detached from the patch cords, returned to its home cage and carted back to the holding room. As criteria for inclusion in OptoPA experiments, during the baseline phases (0–3 min) of the OptoPA test day, mice that spent more than 90% of the time in one single zone were excluded. Additionally, mice that spent 100% of the time in one zone in any 3 min phase of the test were also excluded.

Analysis

Automated OptoPA tracking was done using Noldus EthoVision. Raw data was extracted and analyzed using Microsoft Excel. The difference scores (DS) reported in the main figures were obtained by subtracting the time spent in the target zone during the baseline phase from the average time spent in the target zone during the two on phases. Negative difference scores denote that the preference for the target zone during on phases is lower than the preference during the baseline phase.

Tone Fear Conditioning - (Figure 3C)

Apparatus

Three distinct contexts were employed and were used in different rooms. Context A chambers were 30 X 25 X 33 cm with perspex floors, a transparent square ceilings, red lighting, and scented with 0.25 % benzaldehyde. The ceilings of the Context A chambers were customized to hold a rotary joint (Doric Lenses) the exterior side of which was connected to a patch cord to a 473 nm laser that was controlled by a pulse generator. The interior side of the rotary joint was connected to two 0.32 M patch cords. All mice had patch cords fitted to the fiber implant prior to being placed in Context A. Context B chambers were 29 X 25 X 22 cm with grid floors, opaque triangular ceilings, bright white lighting, and scented with 1 % acetic acid. Context C chambers were 29 X 25 X 22 cm with glossy white plastic floors, no ceilings, dim lighting, and scented with 1 ml citral in a tray underneath.

Habituation

Habituation to Context A was identical to Contextual Fear Conditioning.

Training

Mice were trained in Context B using a tone fear conditioning paradigm. Training sessions were 420 s in duration, and three tone presentations (2 kHz and 75 dB) of 20 s duration were delivered at 180 s, 260 s, and 340 s and co-terminated with a 2 s 0.6 mA shock. SAL or ANI was delivered immediately after training. After fear conditioning, mice were placed in their home cages, and carted back to the holding room. To enable engram labeling, mice were kept on regular food without DOX for 24-30 hours prior to training. When training was complete, mice were switched back to food containing 40 mg kg^{-1} DOX.

Testing

All testing sessions in Context C were 420 s in duration and three tone presentations (2 kHz and 75 dB) of 20 s duration were delivered at 180 s, 260 s, and 340 s. Testing sessions in Context A were 12 min in duration, and were identical to the habituation sessions, consisting of four 3 min epochs, with the first and third epochs as the Light-Off epochs, and the second and fourth epochs as the Light-On epochs. During the Light-On epochs, the mouse received light stimulation for the entire 3 min duration. At the end of the 12 min, the mouse was immediately detached from the patch cords, returned to its home cage and carted back to the holding room.

Contextual Fear Conditioning – Reconsolidation Amnesia - (Figure 4A)

Apparatus, Habituation, and Training procedures used for the reconsolidation experiment were identical to those of the consolidation experiment (above). 1 day post training, contextual fear memory was reactivated by a 3 min re-exposure to the training Context B. SAL or ANI was delivered immediately after context re-exposure. 2 days post-training, amnesia due to disrupting reconsolidation was confirmed by 3 min test session in Context B. 3 days post-training, mice were subjected to a Context A test session consisting of four 3 min epochs, with the first and third epochs as the Light-Off epochs, and the second and fourth epochs as the Light-On epochs. During the Light-On epochs, the mouse received light stimulation (20 Hz) for the entire 3 min duration. At the end of the 12 min, the mouse was immediately detached from the patch cords, returned to its home cage and carted back to the holding room.

Inception of Fear Association - (Figure 4B)

Apparatus

Three distinct contexts were employed and were used in different rooms. Context A chambers were 29 X 25 X 22 cm with black cardboard floors, opaque triangular ceilings, red lighting, and scented with 1 % acetic acid. Context B chambers were 60 X 29 X 30 cm with white Perspex floors, white Perspex walls, no ceilings, bright white lighting, and unscented. The Context C chamber was 30 X 25 X 33 cm were with a metal grid floor, metallic square ceilings, dim white lighting, and scented with 0.25 % benzaldehyde. The ceiling of the Context C chamber was customized to hold a rotary joint (Doric Lenses) the exterior side of which was connected to a patch cord to a 473 nm laser that was controlled by a pulse generator. The interior side of the rotary joint was connected to two 0.32 M patch cords.

Four mice were run simultaneously in four identical Context A chambers. Two mice were run simultaneously in two identical Context B chambers. All experimental groups were counter-balanced for chamber within contexts. Mice were run individually in a single Context C chamber.

Context exposure

Mice were exposure to target Context A for 600 s. SAL or ANI was delivered immediately after context exposure. Immediately after context exposure, mice were placed in their home cages, and carted back to the holding room. To enable engram labeling, mice were kept on regular food without DOX for 24-30 hours prior to training. When training was complete, mice were switched back to food containing 40 mg kg^{-1} DOX.
1 day post-exposure to Context A, all mice were exposed to control Context B for 600 s while on DOX.

Fear Inception

2 days post-exposure to Context A, all mice were subjected to a fear inception procedure in Context C as described in (17). The inception session was 420 s in duration and consisted of 120 s of Light-Off, followed by 300 s of Light-On. Three 0.75 mA shocks of 2 s duration were delivered at 240 s, 300s, and 360 s. At the end of the 420 s, the mouse was immediately detached from the patch cords, returned to its home cage and carted back to the holding room.

Testing

Mice were tested in Context B 4 days post-exposure to Context A, and then tested to Context A 5 days post-exposure to Context A.

Quantification of freezing behavior

All behavioral experiments were analyzed blind to experimental group. Researcher 1 performed behavioral experiments and following the conclusion of each experiment all videos were randomized before manual scoring. Behavioral performance was recorded by digital video camera. For context and tone recall sessions, data were quantified using FreezeFrame software (ActiMetrics) with bout size set at 1.25 ms In the case of fear inception, freezing behavior was manually scored because the dark floor material resulted in inaccurate FreezeFrame data capture. Light stimulation during the habituation and test sessions interfered with the motion detection of the program, and therefore all light-induced freezing behavior was manually quantified by eye. Videos were scored individually, and investigators were blind to experimental condition and test day during all manual scoring.

Behavioral statistics

Data analysis and statistics were conducted using Prism (Graphpad software). Unpaired student's t-tests were used for independent group comparisons, with Welch's correction observed when group variances were significantly different. Paired student's t-tests were used to assess light-induced freezing behavior within groups.

Immunohistochemistry

Mice were dispatched by overdosing with 750–1000 mg kg^{-1} avertin and perfused transcardially with PBS, followed by 4 % paraformaldehyde (PFA) in PBS. Brains were extracted from the skulls and incubated in 4 % PFA at room temperature overnight. Brains were transferred to PBS and 50 μm coronal slices were taken using a vibratome and collected in PBS. For immunostaining, each slice was placed in PBS + 0.2 % Triton X-100 (PBS-T), with 5 % normal goat serum for 1 h and then incubated with primary antibody at 4^{o}C for 24 h. Slices then underwent three wash steps for 10 min each in PBS-T, followed by 1 h incubation with secondary antibody. Slices underwent three more wash steps of 10 min each in PBS-T, followed by mounting and cover-slipping on microscope slides. All imaging and analyses were performed blind to the experimental conditions. Antibodies used for staining were as follows: to stain for ChR2-EYFP, slices were incubated with primary chicken anti-GFP (Life Technologies) (1:1000) and visualized using anti-chicken Alexa-488 (Life Technologies) (1:200). For ChR2-mCherry, slices were

stained using primary rabbit anti-RFP (Rockland) (1:1000) and secondary anti-rabbit Alexa-555 (Life Technologies) (1:200). c-Fos was stained with rabbit anti-c-Fos (1:500, Calbiochem) and anti-rabbit Alexa-568 (Life Technologies) (1:500). Arc was stained with rabbit anti-Arc (1:300, Synaptic Systems) and anti-rabbit Alexa-568 (Life Technologies) (1:500).

Cell counting

All cell counting experiments were conducted blind to experimental group. Researcher 1 trained the animals and administered drug, while Researcher 2 dispatched the animals and conducted cell counting. To quantify the expression pattern of ChR2-EYFP and ChR2-mCherry in SAL and ANI injected c-fos-tTA mice, the number of EYFP/mCherry immunoreactive neurons were counted from 4-5 coronal slices per mouse (n = 3-5 for SAL and ANI groups, respectively). Coronal slices centered on coordinates covered by the optic fiber implants were taken from dorsal hippocampus (–1.82 mm to –2.30 mm AP). Fluorescence images were acquired using a Zeiss AxioImager.Z1/ApoTome microscope (20 X magnification). Automated cell counting analysis was performed using ImageJ software. The cell body layer of DG granule cells (upper blade), CA3 cells or sub-regions of the amygdala (BLA vs. CeA) were outlined as a region of interest (ROI) according to the DAPI signal in each slice. The number of EYFP-/mCherry-positive cells per section was calculated by thresholding EYFP/mCherry immunoreactivity above background levels. For statistical analysis, we used a one-way ANOVA followed by Tukey's multiple comparisons (α = 0.05). Data were analyzed using Microsoft Excel with the Statplus plug-in. All imaging and analyses were performed blind to the experimental conditions. Percentage engram cell reactivation data plotted in Fig. 3E calculated as (($cFos^+$, $ChR2^+$) / (Total $ChR2^+$)) X 100. Total engram cell reactivation was calculated as (($cFos^+$, $ChR2^+$) / (Total $DAPI^+$) X 100. $DAPI^+$ counts were approximation of 5 dorsal DG slices using ImageJ.

Stereotactic injection and optic fiber implant

DG injections of AAV_9-TRE-ChR2-EYFP were targeted bilaterally to (-1.9 mm AP, +/- 1.3 mm ML, –2.0 mm DV). DG implants were placed at (-1.9 mm AP, +/- 1.3 mm ML, –1.85 mm DV). CA3 injections of AAV_9-TRE-mCherry were targeted bilaterally to (-2.0 mm AP, +/- 2.0 mm ML, –1.9 mm DV). BLA injections of AAV_9-TRE-mCherry were targeted bilaterally to (-1.4 mm AP, +/- 3.1 mm ML, –4.6 mm DV). All virus volumes were 300 nl. As criteria we only included mice with ChR2-EYFP expression limited to the targeted region.

Amygdala activation in amnesia - (Figure 5A-C)

Four groups of c-fos-tTA mic e injected with AAV_9-TRE-ChR2-EYFP in the DG along with optic fiber implants were used for this experiment. Memory engram cells for contextual fear conditioning (CFC) were labeled in the DG of all groups. A day after training, two groups of mice (Saline Natural Cues, Anisomycin Natural Cues) were returned to the conditioning context (Context B) for a natural memory recall test followed by timed perfusions; performed to identify recall-induced $cFos^+$ cells. The remaining groups (Saline ChR2, Anisomycin ChR2) were placed in Context A for DG engram activation followed by timed perfusions. By this protocol, we quantified $cFos^+$ neurons in the amygdala (CeA, BLA) following either natural recall or DG engram activation.

Cellular connectivity in amnesia - (Figure 5D-K)

In support of the physiological connectivity data in Figure 1G, four groups of c-fos-tTA mice injected with AAV_9-TRE-ChR2-EYFP in the DG and AAV_9-TRE-mCherry in CA3 and BLA along with optic fiber implants were prepared for this experiment. Memory engram cells for CFC were labeled in DG, CA3 and BLA of all groups. A day after training, two groups of mice (Saline Natural Cues, Anisomycin Natural Cues) were returned to the conditioning context (Context B) for a natural memory recall test followed by timed perfusions. The remaining groups (Saline ChR2, Anisomycin ChR2) were placed in Context A for DG engram activation followed by timed perfusions. This procedure allowed us to quantify the percentage of engram neurons in CA3 and BLA that were re-activated ($cFos^+$) by either natural recall or DG engram activation.

Supplementary Figures

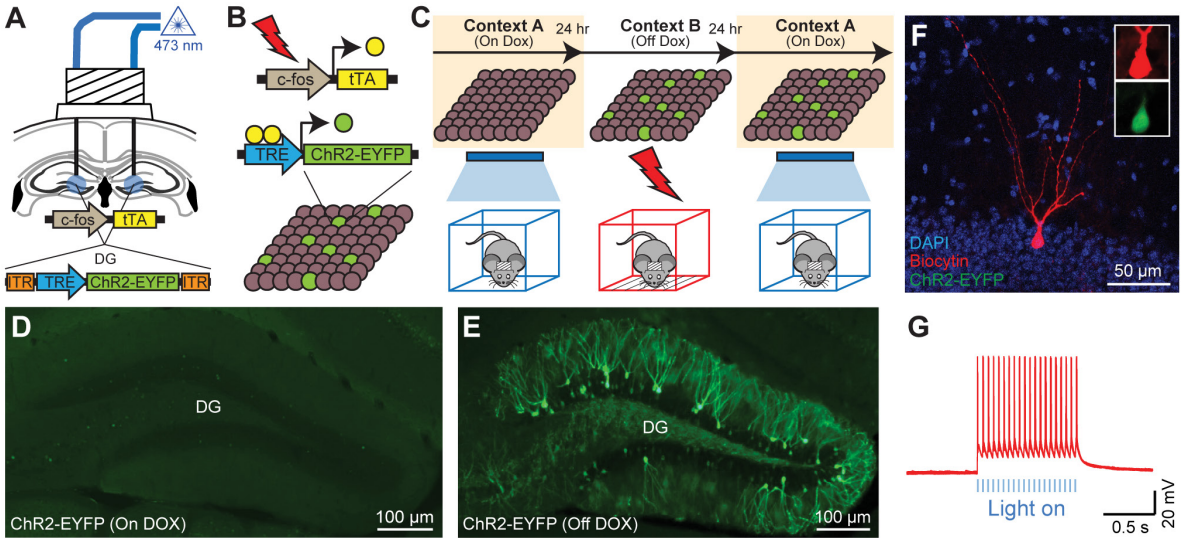

Figure S1: Labeling Dentate Gyrus Engram Cells with ChR2.

(A) Adeno-associated virus carrying *ChR2* gene under the control of a TRE promoter (AAV_9-TRE-ChR2-EYFP) was stereotactically injected in the dentate gyrus (DG) of c-fos-tTA transgenic mice. Following virus injections, bilateral optic fibers were implanted into the DG.

(B) When the *c-fos* promoter is active, tTA is expressed in cells. tTA protein binds to the TRE promoter, resulting in the expression of ChR2-EYFP. DOX prevents binding of tTA to the TRE promoter, restricting expression of ChR2 to defined temporal windows.

(C) Naïve, unlabeled mice were habituated to the patch cord and laser in Context A while On DOX. Mice were taken Off DOX 24-30 hours prior to CFC in Context B. Mice were placed back On DOX immediately after training. DG engrams were evoked by blue laser stimulation of the DG in Context A, at least 24 hours after training.

(D) Representative image showing a DG section from a c-fos-tTA mouse injected with AAV_9-TRE-ChR2-EYFP that was kept On DOX during training. No significant expression of ChR2-EYFP was observed, demonstrating DOX control over the labeling method.

(E) Representative image showing a DG section from a c-fos-tTA mouse injected with AAV_9-TRE-ChR2-EYFP, Off DOX from 24 hours before training. Sparse ChR2-EYFP expression occurs across the DG.

(F) Representative image of a ChR2-EYFP labeled DG neuron injected with biocytin during patch clamp recording.

(G) Blue light stimulation (20 pulses, 20 Hz, 15 ms each) of ChR2-EYFP labeled DG neuron resulted in spikes.

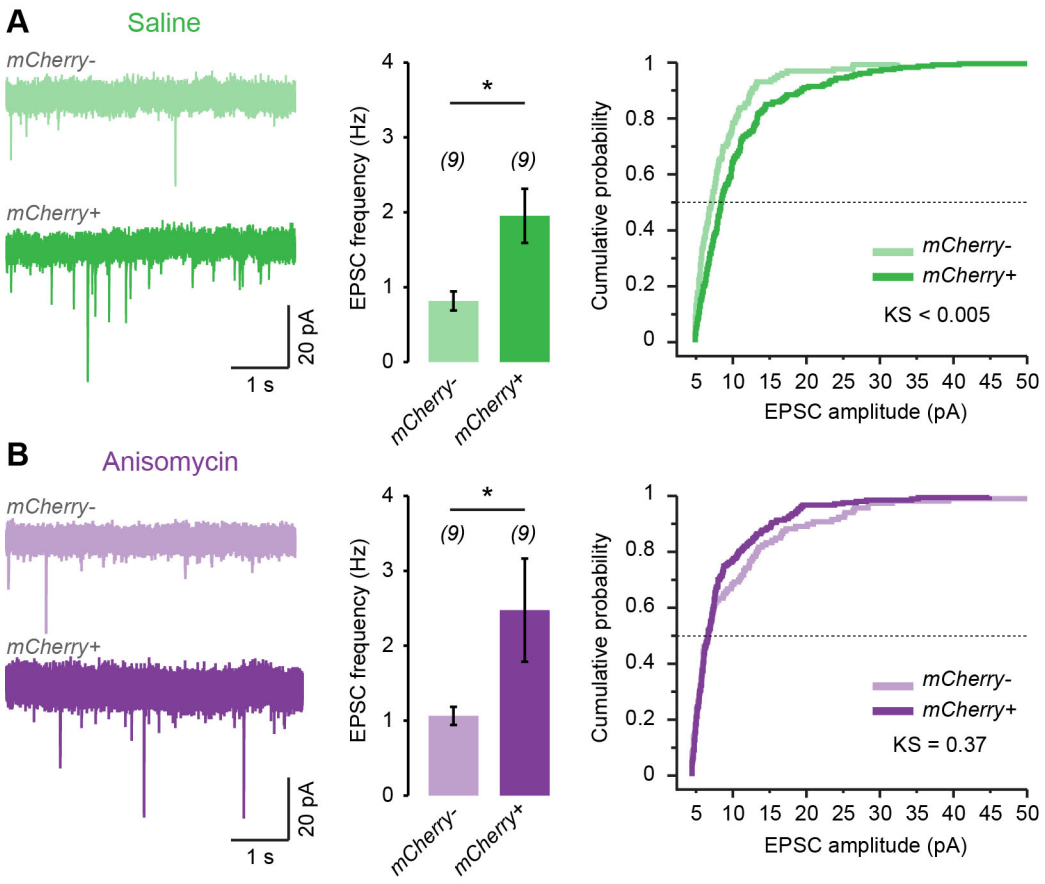

Figure S2: Analysis of Spontaneous EPSCs.

(A) Example of spontaneous EPSC recordings from mCherry$^-$ and mCherry$^+$ DG granule cells collected from cfos-tTA mice injected with AAV$_9$-TRE-mCherry in DG (same cells of Fig. 1A-E). Mice were injected with saline immediately after CFC and sacrificed 24 hr later for *ex vivo* recording. The mCherry$^+$ group displays higher EPSC frequency (two tailed paired t-test, $P < 0.05$) and higher EPSC amplitude than the mCherry$^-$ group (Kolmogorov-Smirnov test, $P < 0.005$).

(B) Example of spontaneous EPSC recordings from mCherry$^-$ and mCherry$^+$ DG granule cells collected from cFos-tTa mice injected either with AAV$_9$-TRE-mCherry in the DG. Mice were injected with anisomycin immediately after CFC and sacrificed 24 hr later for *ex vivo* recording. The mCherry$^+$ group displays higher EPSC frequency than the mCherry$^-$ group (two tailed paired t-test, $P < 0.05$) but the distributions of EPSC amplitudes are similar (Kolmogorov-Smirnov test, $P = 0.37$).

The mCherry$^+$ cells of the saline group display higher EPSC amplitudes than the mCherry$^+$ cells of the anisomycin group (Kolmogorov-Smirnov test, $P < 0.001$), whereas the mCherry$^-$ cells of the saline and the anisomycin group display similar EPSC amplitudes (Kolmogorov-Smirnov test, $P = 0.12$).

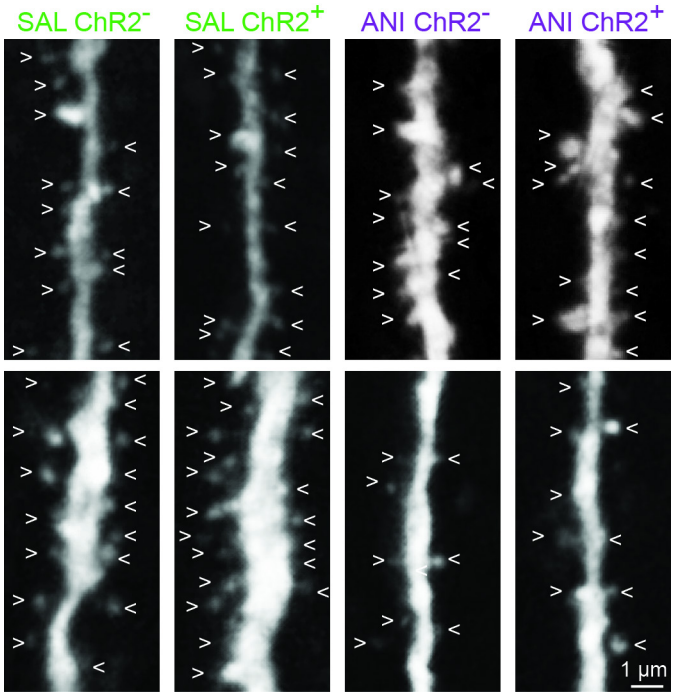

Figure S3: Confocal Images of Dendritic Spines.

Two series (top and bottom) of confocal images of dendritic spines form $ChR2^+$ and $ChR2^-$ DG granule cell dendrites from the Saline (SAL) or the Anisomycin (ANI) group. Scale bar is the same for all the images.

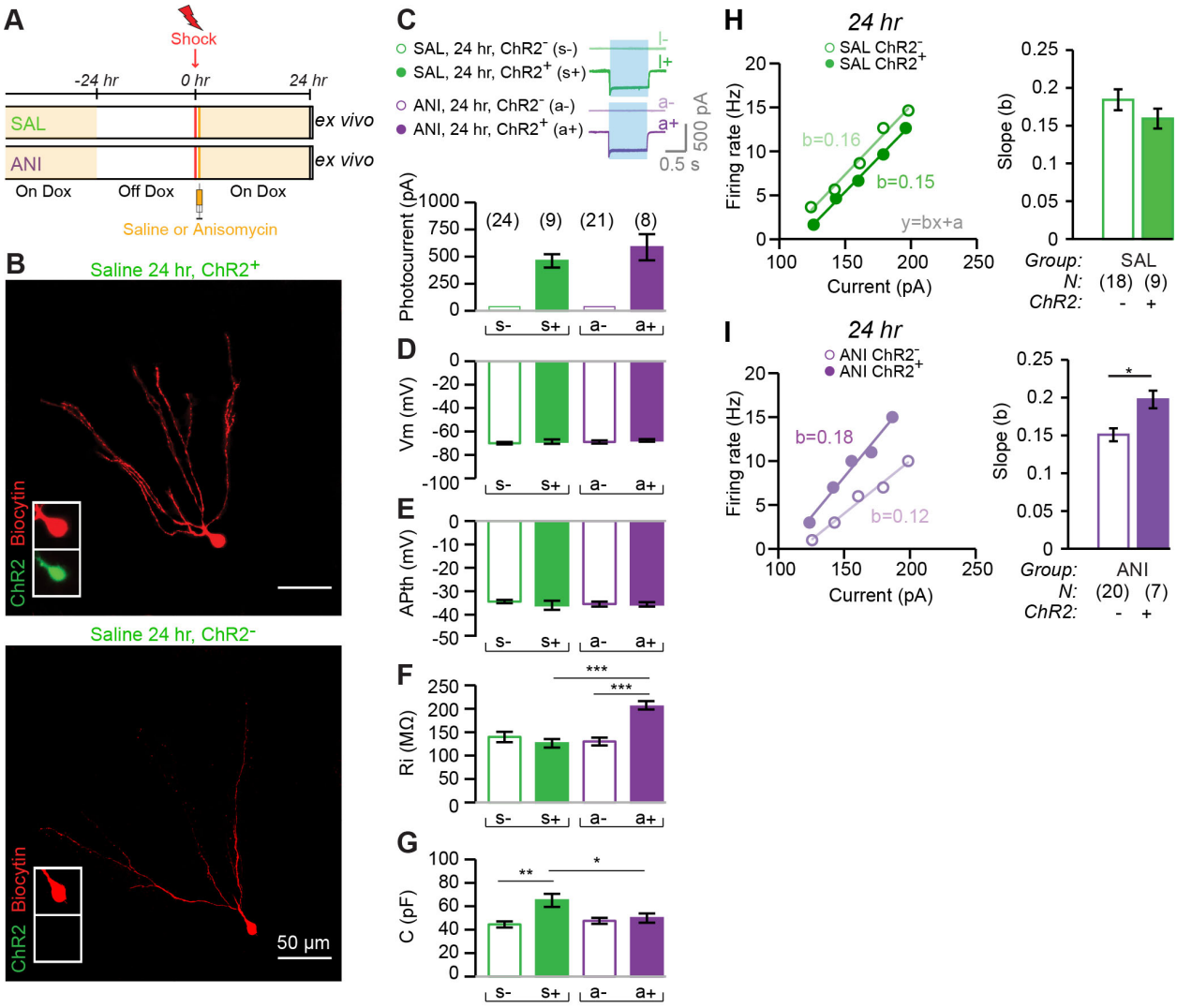

Figure S4: Physiological Profiling of DG Engram Cells.

(A) Schematic of *ex vivo* physiological experiments. c-fos-tTA mice with AAV_9-TRE-ChR2-EYFP injected into the DG were taken Off DOX 24 hrs before CFC, administered either SAL or ANI, and dispatched 24 hrs post-training,

(B) Representative images of $ChR2^+$ and $ChR2^-$ DG cells taken from the SAL group.

(C-I) Intrinsic physiological properties of engram ($ChR2^+$) and non-engram ($ChR2^-$) cells of the SAL (green), and ANI (purple) groups.

(C) Photocurrent measurements (pA) for $ChR2^+$ and $ChR2^-$ cells. Traces are displayed above bar charts. Blue light evoked comparable current influx in $ChR2^+$ cells but not in $ChR2^-$ cells of all three groups. Cell numbers in parentheses.

(D) Resting membrane potential measurements (Vm) for $ChR2^+$ and $ChR2^-$ cells across groups

(E) Action potential threshold (APth) for $ChR2^+$ and $ChR2^-$ cells across groups.

(F) Input resistance (Ri) for $ChR2^+$ and $ChR2^-$ cells across groups.

(G) Membrane capacitance (C) for $ChR2^+$ and $ChR2^-$ cells across groups.

(H, I) Examples of relationship between current injection and firing rate for the SAL (H) and ANI (I) groups, for engram $ChR2^+$ and non-engram $ChR2^-$ cells. Data are approximated by linear fit (gray formula in H) and the average value of the slope (b) is displayed in the bar charts. The $ChR2^+$ cells from the SAL group (H) display an excitability level similar to $ChR2^-$ cells. The $ChR2^+$ cells from the ANI group (I) display a significant 31% increase in excitability compared to $ChR2^-$ cells.

Data are represented as mean ± SEM. Statistical comparison are performed by using unpaired t tests, * $p < 0.05$, ** $p < 0.05$, and *** $p < 0.001$.

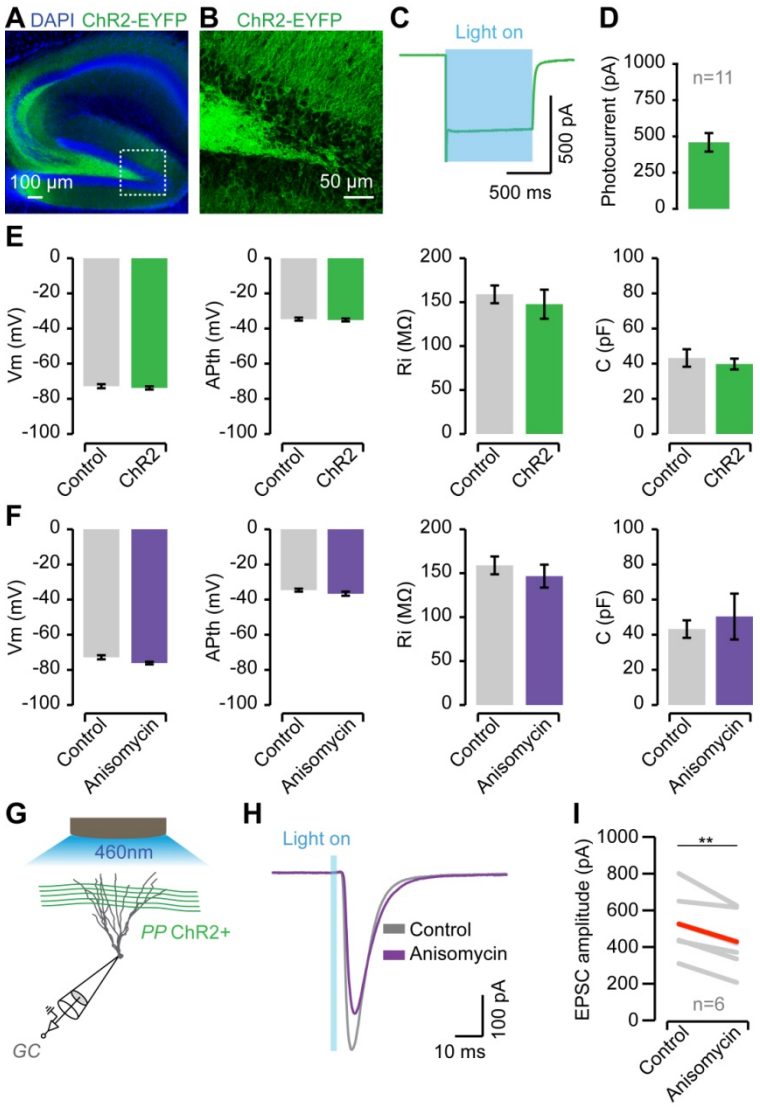

Figure S5: ChR2 and ANI have no Effect on the Intrinsic Properties of DG Granule Cells.

(A-B) The DG of c-fos-tTA transgenic mice were infected using an AAV_8-CaMKIIα-ChR2-EYFP virus. B, from the dotted-line box in A).

(C-D) Optogenetic stimulation of DG cells during voltage clamp recording revealed a robust photocurrent comparable to what was previously shown in fig. S4C.

(E) ChR2 expression had no effect on the intrinsic properties (resting membrane potential Vm, action potential threshold APth, input resistance Ri and capacitance C) of DG cells ($ChR2^+$ cells n = 11, $ChR2^-$ cells n = 16).

(F) Direct bath application of 40 µM ANI had no effect on the intrinsic properties of DG cells (control n = 11, ANI n = 14).

(G) Voltage clamp recording of a DG cell combined with optogenetic stimulation of $ChR2^+$ axons of the perforant path.

(H) Examples of excitatory postsynaptic currents (EPSCs) recorded in DG cells responding to optogenetic stimulation of the $ChR2^+$ axons of the perforant path in control conditions and following ANI bath application. Note the mild difference.

(I) Average EPSCs of experiments described in panel G-H ($n = 6$, paired t test ** $p < 0.01$).

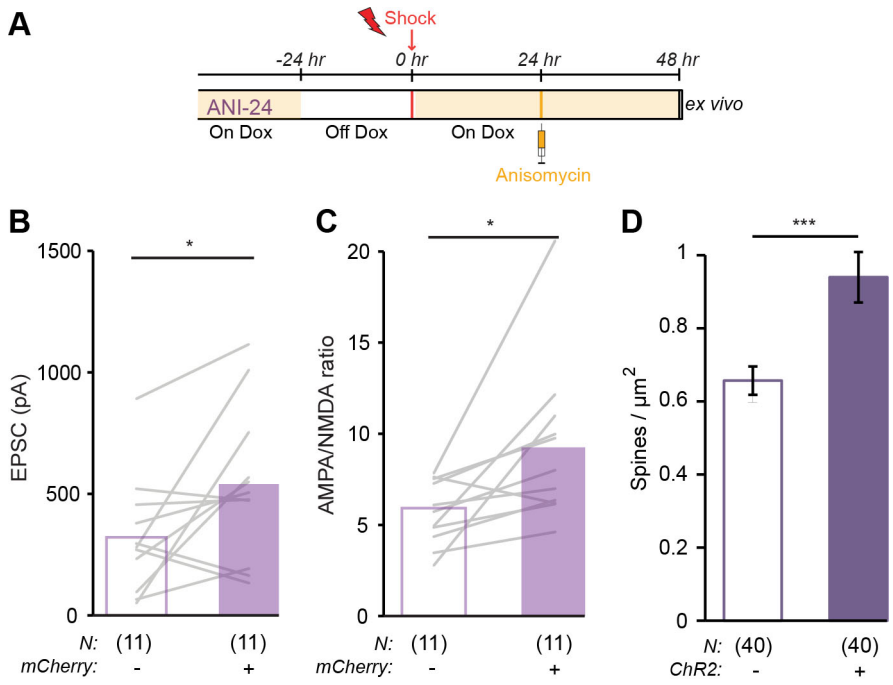

Figure S6: Anisomycin Injection Outside of the Memory Consolidation Window does not Affect Synaptic Strength, AMPA/NMDA Receptor Current Ratio, or Dendritic Spine Density.

(A) cfos-tTA mice injected in the DG either with AAV_9-TRE-mCherry (for synaptic analysis) or AAV_9-TRE-ChR2-EYFP (for spine density analysis) were taken off DOX 24 hr before exposure to contextual fear conditioning, injected with anisomycin 24 hr later and then sacrificed 24 hr after injection for *ex vivo* recording.

(B) Analysis of synaptic strength. The $mCherry^+$ group displays higher synaptic strength than the $mCherry^-$ group (two tailed paired t-test, $P < 0.05$).

(C) Analysis of AMPA/NMDA receptors ratio. The $mCherry^+$ group displays higher AMPA/NMDA receptors ratio than the $mCherry^-$ group (two tailed paired t-test, $P < 0.05$).

(D) Dendritic spine density analysis of $ChR2^+$ and $ChR2^-$ DG granule cells. The $ChR2^+$ group displays higher spine density than the $ChR2^-$ group (two tailed unpaired t-test, $P < 0.001$).

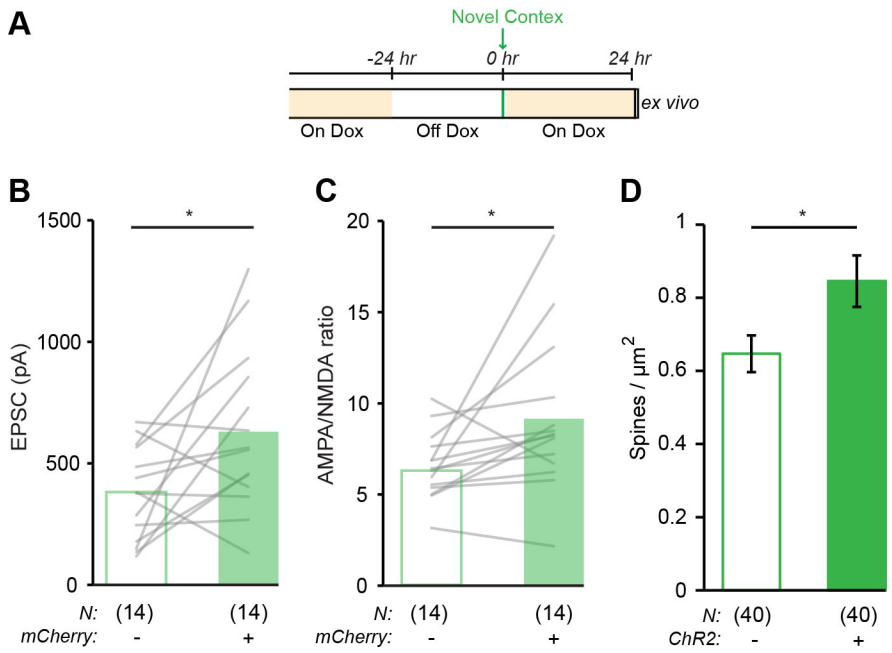

Figure S7: Effect of Exposure to Novel Context on Synaptic Strength, AMPA/NMDA Receptors Current Ratio, and Dendritic Spine Density.

(A) cfos-tTA mice injected in DG either with AAV_9-TRE-mCherry (for synaptic analysis) or AAV_9-TRE-ChR2-EYFP (for spine density analysis) were taken off DOX 24 hr before a 5 min. exposure to a novel context and then sacrificed 24 hr later for ex vivo recording.

(B) Analysis of synaptic strength. The $mCherry^+$ group displays higher synaptic strength than the $mCherry^-$ group (two tailed paired t-test, $P < 0.05$).

(C) Analysis of AMPA/NMDA receptors ratio. The $mCherry^+$ group displays higher AMPA/NMDA receptors ratio than the $mCherry^-$ group (two tailed paired t-test, $P < 0.05$).

(D) Dendritic spine density analysis of $ChR2^+$ and $ChR2^-$ DG granule cells. The $ChR2^+$ group displays higher spine density than the $ChR2^-$ group (two tailed unpaired t-test, $P < 0.05$).

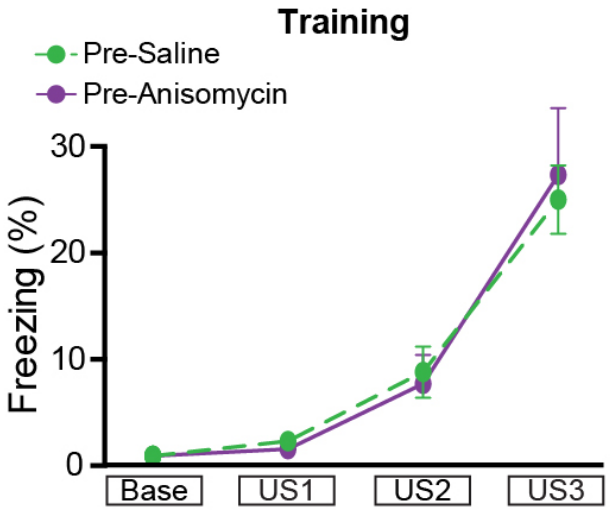

Figure S8: Response to Shock During CFC.

For the DG consolidation experiment (Fig. 2), naïve implanted c-fos-tTA mice were subjected to a CFC protocol while Off DOX, where three 0.75 mA shocks (unconditioned stimulus US1-3) of 2 s duration were delivered at 150 s, 210 s, and 270 s. No difference in unconditioned freezing behavior was observed between the two groups.

Data presented as mean ± SEM.

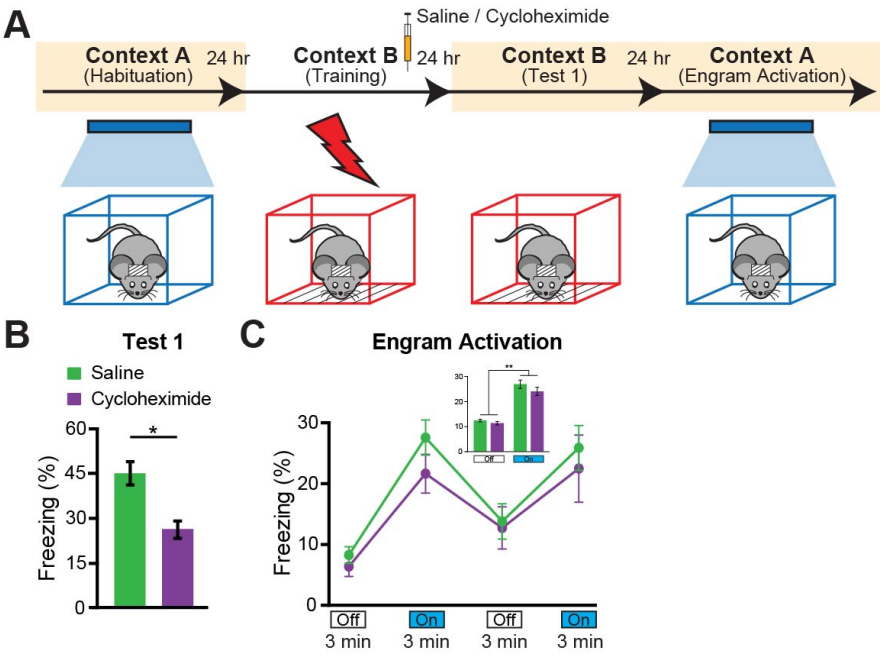

Figure S9: Optogenetic Stimulation of DG Engram Cells Retrieves fear memory in CHM-Induced Retrograde Amnesia.

(A) Schematic of the behavioral schedule used for experiments.

(B) Long-term memory recall in Context B, 1 day post-training. CHM group (N = 9) displayed significantly less freezing behavior to natural contextual cues than the SAL group (N = 9), ($p < 0.04$).

(C) Light-induced memory recall in Context A, 2 days post-training with Light-Off and Light-On epochs. Freezing levels for the two Light-Off and Light-On epochs are further averaged in the inset. Significant freezing due to light stimulation was observed in both the SAL ($p < 0.001$) and CHM groups ($p < 0.01$). Light-induced freezing levels did not differ between groups.

Data presented as mean ± SEM.

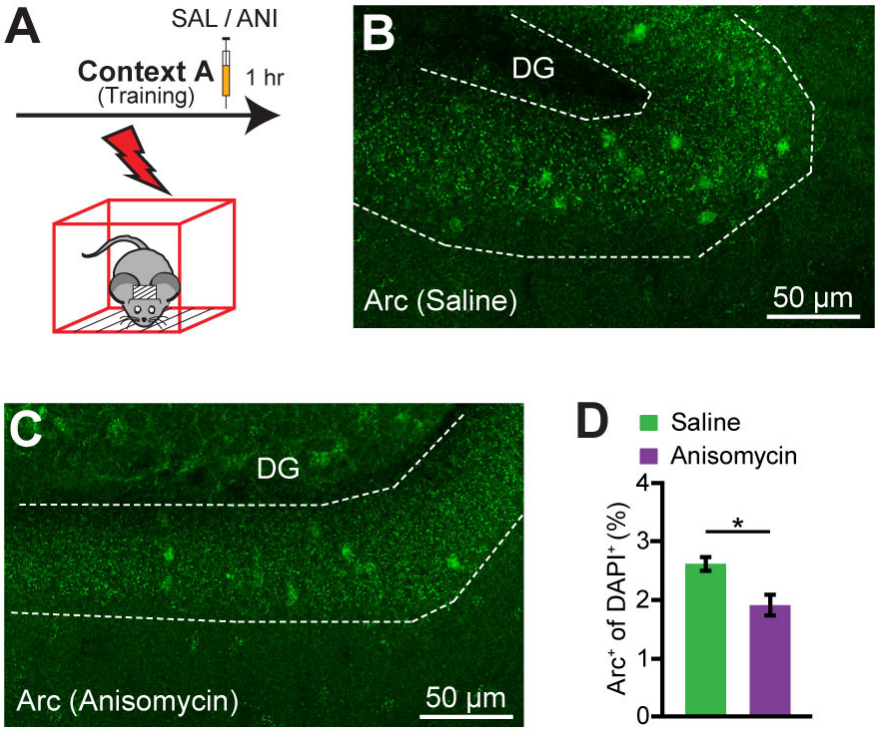

Figure S10: Post-Training Anisomycin Impairs DG Protein Synthesis.

(A) Schematic of the behavioral schedule used for experiments. Mice were pefused 1 hour post-training.

(B) Representative image of Arc staining in the DG of mice treated with saline.

(C) Representative image of Arc staining in the DG of mice treated with anisomycin.

(D) Average percentages of Arc^+ DG cells of SAL and ANI groups.

Data presented as mean ± SEM, * $p < 0.05$.

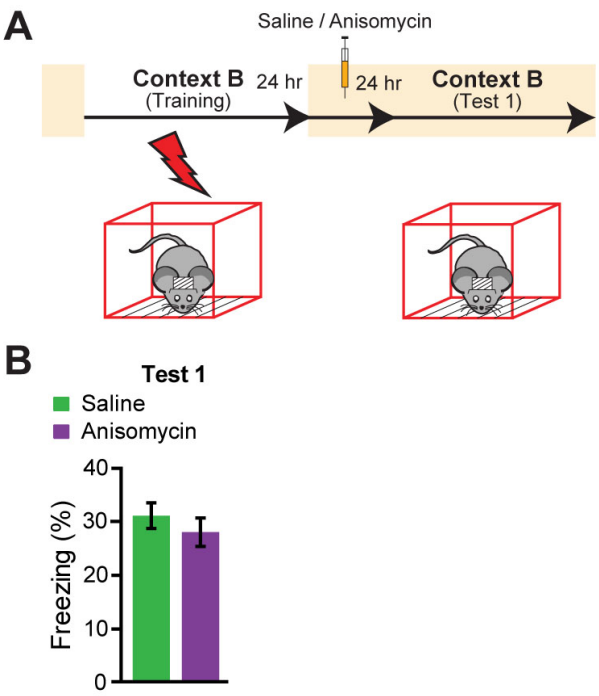

Figure S11: Anisomycin Delivery 24 hours Post-Training did not Induce Retrograde Amnesia.

(A) Schematic of the behavioral schedule used for experiments.

(B) Long-term memory recall in Context B, 1 day post-drug treatment. ANI group (N = 11) displayed equivalent freezing behavior to SAL group (N = 11).

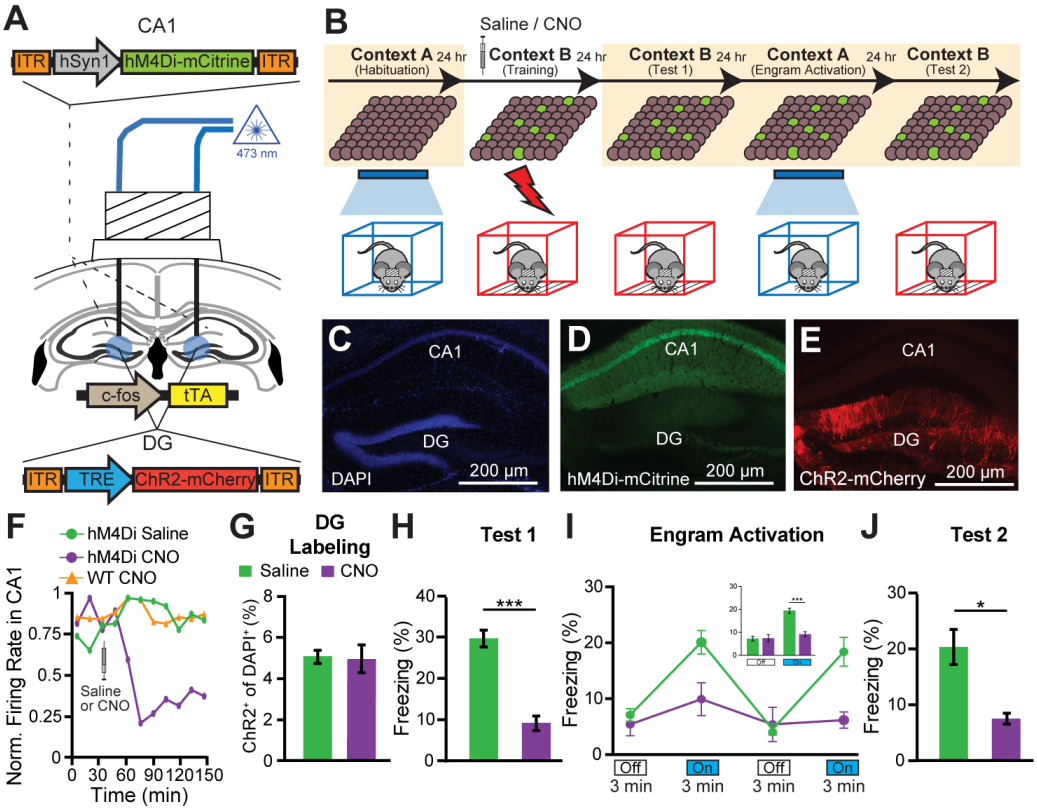

Figure S12: Optogenetic Stimulation of Engram Cells Does Not Retrieve Fear Memory following Anterograde Amnesia due to Impaired Encoding.

(A) An AAV virus carrying the inhibitory DREADDs hM4Di receptor under the control of a hSyn1 promoter (AAV_9-hSyn1-hM4Di-mCitrine) was stereotactically injected in CA1 of c-fos-tTA transgenic mice, with AAV_9-TRE-ChR2-mCherry injected into the DG. Following virus injections, bilateral optic fibers were implanted into DG.

(B) Schematic of the behavioral schedule used for memory encoding experiment. Depictions of DG cell populations. Mice were taken off 24-30 hrs before contextual fear conditioning in Context B and SAL or CNO (5 mg kg^{-1}) 1 hr before training.

(C-E) Representative images showing a hippocampal section from a c-fos-tTA mouse expressing hM4Di-mCitrine in CA1, and ChR2-mCherry in DG.

(F) CNO administration triggered hM4Di receptors to inhibit CA1 neuronal firing.

(G) $ChR2^+$ cell counts from DG sections of SAL (n = 4) and CNO (n = 4) treated c-fos-tTA mice. CNO treatment did not impair ChR2 labeling of DG engram cells.

(H) Long-term memory recall in Context B, 1 day post-training. The CNO group (N = 13) showed significantly less freezing behavior than the SAL group (N = 11), ($p < 0.001$).

(I) Light-induced memory recall in Context A, 2 days post-training with Light-Off and Light-On epochs. Freezing levels for the two Light-Off and Light-On epochs are further averaged in the inset. Significant freezing due to light stimulation was observed in both the SAL ($p < 0.0001$) and CNO groups ($p < 0.05$). Light-induced freezing was significantly lower in the CNO group (18.2% ± 1.3% versus 9.3% ± 1.6% freezing; $p < 0.0005$).

(J) Long-term memory recall in Context B, 3 days post-training. The CNO group showed significantly less freezing behavior than the SAL group (20.7% ± 4.7% versus 8.9% ± 1.7% freezing; $p < 0.05$).

Data presented as mean ± SEM.

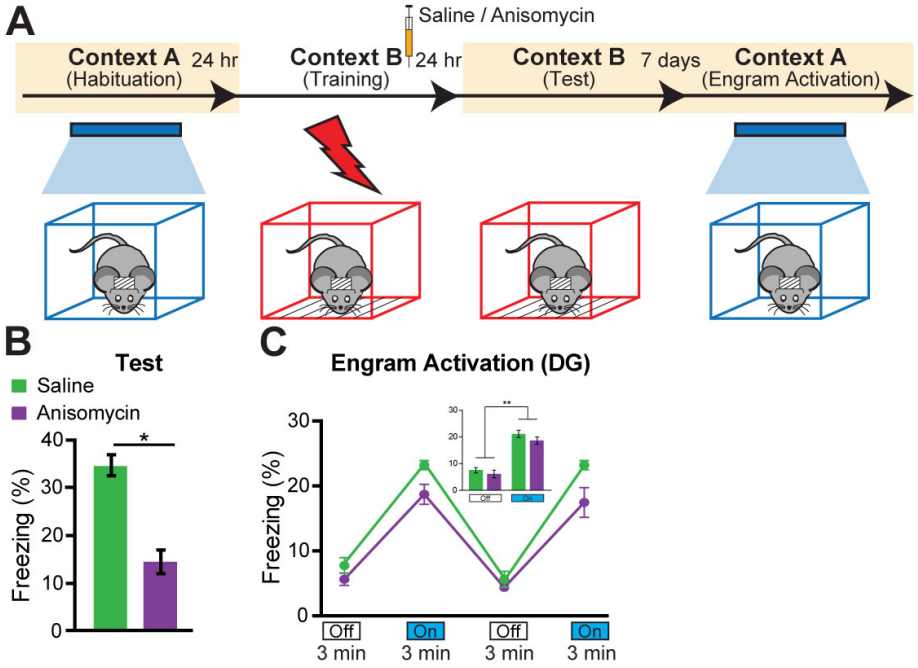

Figure S13: Optogenetic Stimulation of DG Engram Cells Retrieves Fear Memory 8 Days After Impaired Consolidation

(A) Schematic of the behavioral schedule used for experiments.

(B) Long-term memory recall in Context B, 1 day post-training. ANI group (N = 8) displayed less freezing behavior to natural contextual cues than the SAL group (N = 7, $p = 0.015$).

(C) Light-induced memory recall in Context A, 8 days post-training with Light-Off and Light-On epochs. Freezing levels for the two Light-Off and Light-On epochs are further averaged in the inset. Significant freezing due to light stimulation was observed in both the SAL ($p < 0.005$) and ANI groups ($p < 0.005$). Light-induced freezing levels did not differ between groups.

Data presented as mean ± SEM.

References and Notes

1. G. E. Müller, A. Pilzecker, *Z. Psychol* **1**, 1–288 (1900).

2. C. P. Duncan, The retroactive effect of electroshock on learning. *J. Comp. Physiol. Psychol.* **42**, 32–44 (1949). Medline doi:10.1037/h0058173

3. J. L. McGaugh, Memory—A century of consolidation. *Science* **287**, 248–251 (2000). Medline doi:10.1126/science.287.5451.248

4. J. B. Flexner, L. B. Flexner, E. Stellar, Memory in mice as affected by intracerebral puromycin. *Science* **141**, 57–59 (1963). Medline doi:10.1126/science.141.3575.57

5. L. B. Flexner, J. B. Flexner, R. B. Roberts, Memory in mice analyzed with antibiotics. Antibiotics are useful to study stages of memory and to indicate molecular events which sustain memory. *Science* **155**, 1377–1383 (1967). Medline doi:10.1126/science.155.3768.1377

6. H. P. Davis, L. R. Squire, Protein synthesis and memory: A review. *Psychol. Bull.* **96**, 518–559 (1984). Medline doi:10.1037/0033-2909.96.3.518

7. E. R. Kandel, The molecular biology of memory storage: A dialogue between genes and synapses. *Science* **294**, 1030–1038 (2001). Medline doi:10.1126/science.1067020

8. R. J. Kelleher 3rd, A. Govindarajan, S. Tonegawa, Translational regulatory mechanisms in persistent forms of synaptic plasticity. *Neuron* **44**, 59–73 (2004). Medline doi:10.1016/j.neuron.2004.09.013

9. T. Takeuchi, A. J. Duszkiewicz, R. G. Morris, The synaptic plasticity and memory hypothesis: Encoding, storage and persistence. *Philos. Trans. R. Soc. Lond. B Biol. Sci.* **369**, 20130288 (2014). Medline

10. A. Govindarajan, I. Israely, S. Y. Huang, S. Tonegawa, The dendritic branch is the preferred integrative unit for protein synthesis-dependent LTP. *Neuron* **69**, 132–146 (2011). Medline doi:10.1016/j.neuron.2010.12.008

11. M. Krug, B. Lössner, T. Ott, Anisomycin blocks the late phase of long-term potentiation in the dentate gyrus of freely moving rats. *Brain Res. Bull.* **13**, 39–42 (1984). Medline doi:10.1016/0361-9230(84)90005-4

12. U. Frey, M. Krug, K. G. Reymann, H. Matthies, Anisomycin, an inhibitor of protein synthesis, blocks late phases of LTP phenomena in the hippocampal CA1 region in vitro. *Brain Res.* **452**, 57–65 (1988). Medline doi:10.1016/0006-8993(88)90008-X

13. Y. Y. Huang, P. V. Nguyen, T. Abel, E. R. Kandel, Long-lasting forms of synaptic potentiation in the mammalian hippocampus. *Learn. Mem.* **3**, 74–85 (1996). Medline doi:10.1101/lm.3.2-3.74

14. R. Semon, *Die Mneme als erhaltendes Prinzip im Wechsel des organischen Geschehens* (Wilhelm Engelmann, Leipzig, 1904).

15. S. A. Josselyn, Continuing the search for the engram: Examining the mechanism of fear memories. *J. Psychiatry Neurosci.* **35**, 221–228 (2010). Medline doi:10.1503/jpn.100015

16. X. Liu, S. Ramirez, P. T. Pang, C. B. Puryear, A. Govindarajan, K. Deisseroth, S. Tonegawa, Optogenetic stimulation of a hippocampal engram activates fear memory recall. *Nature* **484**, 381–385 (2012). Medline

17. S. Ramirez, X. Liu, P. A. Lin, J. Suh, M. Pignatelli, R. L. Redondo, T. J. Ryan, S. Tonegawa, Creating a false memory in the hippocampus. *Science* **341**, 387–391 (2013). Medline doi:10.1126/science.1239073

18. R. L. Redondo, J. Kim, A. L. Arons, S. Ramirez, X. Liu, S. Tonegawa, Bidirectional switch of the valence associated with a hippocampal contextual memory engram. *Nature* **513**, 426–430 (2014). Medline doi:10.1038/nature13725

19. C. A. Denny, M. A. Kheirbek, E. L. Alba, K. F. Tanaka, R. A. Brachman, K. B. Laughman, N. K. Tomm, G. F. Turi, A. Losonczy, R. Hen, Hippocampal memory traces are differentially modulated by experience, time, and adult neurogenesis. *Neuron* **83**, 189–201 (2014). Medline doi:10.1016/j.neuron.2014.05.018

20. K. Z. Tanaka, A. Pevzner, A. B. Hamidi, Y. Nakazawa, J. Graham, B. J. Wiltgen, Cortical representations are reinstated by the hippocampus during memory retrieval. *Neuron* **84**, 347–354 (2014). Medline doi:10.1016/j.neuron.2014.09.037

21. K. K. Cowansage, T. Shuman, B. C. Dillingham, A. Chang, P. Golshani, M. Mayford, Direct reactivation of a coherent neocortical memory of context. *Neuron* **84**, 432–441 (2014). Medline doi:10.1016/j.neuron.2014.09.022

22. L. G. Reijmers, B. L. Perkins, N. Matsuo, M. Mayford, Localization of a stable neural correlate of associative memory. *Science* **317**, 1230–1233 (2007). Medline doi:10.1126/science.1143839

23. R. L. Clem, R. L. Huganir, Calcium-permeable AMPA receptor dynamics mediate fear memory erasure. *Science* **330**, 1108–1112 (2010). Medline doi:10.1126/science.1195298

24. A. Suzuki, S. A. Josselyn, P. W. Frankland, S. Masushige, A. J. Silva, S. Kida, Memory reconsolidation and extinction have distinct temporal and biochemical signatures. *J. Neurosci.* **24**, 4787–4795 (2004). Medline doi:10.1523/JNEUROSCI.5491-03.2004

25. B. N. Armbruster, X. Li, M. H. Pausch, S. Herlitze, B. L. Roth, Evolving the lock to fit the key to create a family of G protein-coupled receptors potently activated by an inert ligand. *Proc. Natl. Acad. Sci. U.S.A.* **104**, 5163–5168 (2007). Medline doi:10.1073/pnas.0700293104

26. J. H. Han, S. A. Kushner, A. P. Yiu, H. L. Hsiang, T. Buch, A. Waisman, B. Bontempi, R. L. Neve, P. W. Frankland, S. A. Josselyn, Selective erasure of a fear memory. *Science* **323**, 1492–1496 (2009). Medline doi:10.1126/science.1164139

27. J. R. Misanin, R. R. Miller, D. J. Lewis, Retrograde amnesia produced by electroconvulsive shock after reactivation of a consolidated memory trace. *Science* **160**, 554–555 (1968). Medline doi:10.1126/science.160.3827.554

28. K. Nader, G. E. Schafe, J. E. Le Doux, Fear memories require protein synthesis in the amygdala for reconsolidation after retrieval. *Nature* **406**, 722–726 (2000). Medline doi:10.1038/35021052

29. X. Liu, S. Ramirez, S. Tonegawa, Inception of a false memory by optogenetic manipulation of a hippocampal memory engram. *Philos. Trans. R. Soc. Lond. B Biol. Sci.* **369**, 20130142 (2014). Medline doi:10.1098/rstb.2013.0142

30. A. Besnard, S. Laroche, J. Caboche, Comparative dynamics of MAPK/ERK signalling components and immediate early genes in the hippocampus and amygdala following contextual fear conditioning and retrieval. *Brain Struct. Funct.* **219**, 415–430 (2014). Medline doi:10.1007/s00429-013-0529-3

31. J. Hall, K. L. Thomas, B. J. Everitt, Fear memory retrieval induces CREB phosphorylation and Fos expression within the amygdala. *Eur. J. Neurosci.* **13**, 1453–1458 (2001). Medline doi:10.1046/j.0953-816x.2001.01531.x

32. J. L. McGaugh, Time-dependent processes in memory storage. *Science* **153**, 1351–1358 (1966). Medline doi:10.1126/science.153.3742.1351

33. Y. Dudai, The neurobiology of consolidations, or, how stable is the engram? *Annu. Rev. Psychol.* **55**, 51–86 (2004). Medline doi:10.1146/annurev.psych.55.090902.142050

34. J. P. Johansen, C. K. Cain, L. E. Ostroff, J. E. LeDoux, Molecular mechanisms of fear learning and memory. *Cell* **147**, 509–524 (2011). Medline doi:10.1016/j.cell.2011.10.009

35. R. R. Miller, L. D. Matzel, Retrieval failure versus memory loss in experimental amnesia: Definitions and processes. *Learn. Mem.* **13**, 491–497 (2006). Medline doi:10.1101/lm.241006

36. C. A. Miller, J. D. Sweatt, Amnesia or retrieval deficit? Implications of a molecular approach to the question of reconsolidation. *Learn. Mem.* **13**, 498–505 (2006). Medline doi:10.1101/lm.304606

37. S. Chen *et al*., *eLife* **3**, e02844 (2014).

38. S. Nabavi, R. Fox, C. D. Proulx, J. Y. Lin, R. Y. Tsien, R. Malinow, Engineering a memory with LTD and LTP. *Nature* **511**, 348–352 (2014). Medline doi:10.1038/nature13294

39. D. O. Hebb, *The Organization of Behavior; A Neuropsychological Theory* (Wiley, New York, 1949).

40. S. Daumas, J. Sandin, K. S. Chen, D. Kobayashi, J. Tulloch, S. J. Martin, D. Games, R. G. Morris, Faster forgetting contributes to impaired spatial memory in the PDAPP mouse: Deficit in memory retrieval associated with increased sensitivity to interference? *Learn. Mem.* **15**, 625–632 (2008). Medline doi:10.1101/lm.990208

41. E. S. Boyden, F. Zhang, E. Bamberg, G. Nagel, K. Deisseroth, Millisecond-timescale, genetically targeted optical control of neural activity. *Nat. Neurosci.* **8**, 1263–1268 (2005). Medline doi:10.1038/nn1525